

Application of the Lagrange mesh method in continuum-discretized coupled-channels calculations

Wendi Chen¹, Hairui Guo², Weili Sun², Tao Ye², Yangjun Ying² and Yinlu Han³

¹ School of Physics, Beihang University, Beijing 100191, China

² Institute of Applied Physics and Computational Mathematics, Beijing 100094, China

³ Key Laboratory of Nuclear Data, China Institute of Atomic Energy, Beijing 102413, China

E-mail: guo_hairui@iapcm.ac.cn

22 September 2021

Abstract. We apply the Lagrange mesh method to discretize continuum states of weakly bound nuclei for continuum-discretized coupled-channels (CDCC) calculations of three-body breakup reactions. This discretization method is compared with the momentum bin method, which is regarded as the standard continuum discretization method, for the reactions $d+^{58}\text{Ni}$ at 80 MeV, $^6\text{Li}+^{40}\text{Ca}$ at 156 MeV and $^6\text{Li}+^{208}\text{Pb}$ at 33.0 MeV. The finite-difference method based on Numerov algorithm is used to solve the coupled channels equations, which permits fast integration of equations. In all cases, the combination of the Lagrange mesh method shows high efficiency and accuracy for the CDCC calculations of the elastic scattering and breakup reactions, especially when the incident energy is around the coulomb barrier.

1. Introduction

The continuum-discretized coupled-channels (CDCC) method is a powerful tool to investigate the reaction mechanisms of weakly bound nuclei induced reactions, which are influenced significantly by the coupling to the continuum states [1]. Although it is originally designed to describe deuteron-nucleus reactions [2], CDCC has been the most accurate and successful method to study the breakup reactions induced by heavy weakly bound nuclei, as it can provide a solution which is very close to the exact three-body wave function [3, 4]. Nowadays CDCC has been extensively applied in the studies of elastic scattering [5, 6], polarization potential [7], breakup reaction [8] and fusion reaction [9] for the nuclear reactions induced by weakly bound nuclei. Some researches based on CDCC framework for a further description of the reactions have been published, such as four body CDCC [10], extended CDCC including the effect of core excitation [11] or target excitation [12].

CDCC solves three body problem by projecting the full wave function onto the model space expanded by a set of discretized internal wave functions of the weakly bound nucleus. Therefore it is an important issue in CDCC that the continuum states should be well represented by a finite number of discrete states. There are two kind of discretization methods so far. One is the momentum bin method [13, 14], which generates the discrete state wave functions by averaging the exact scattering wave functions within the intervals of momentum or energy. Its result can be used as the benchmark for CDCC calculation. Besides, there is an effective way to provide the discrete state wave functions via diagonalizing the internal Hamiltonian of the weakly bound nucleus with a set of square-integrable basis functions. This way is called the pseudo-state (PS) method. However there is a large amount of calculation in CDCC with the above methods because of the numerical integration for coupling matrix elements.

Careful investigation of inelastic breakup reactions requires the coupling of many discretized states of the projectile and some excited states of the target nucleus, which will be very complex. Therefore, it is important to promote the efficiency of the CDCC calculation. In the present work, the Lagrange mesh method is applied to discretize the continuum states of weakly bound nuclei and calculate their bound states. With this method, the CDCC coupling matrix elements can be calculated by Gauss-quadrature approximation, which reduces the amount of calculation remarkably. The validity of applying Lagrange mesh method in CDCC has been verified by T. Druet et al. [15] for $d(p+n)+^{58}\text{Ni}$ at incident energy of 80 MeV in laboratory system (EL) and by T. Druet and P. Descouvemont [16] for $^{11}\text{Be}(^{10}\text{Be}+n)+^{64}\text{Zn}$ at incident energy of 24.5 MeV in center of mass system. However, in their studies, the CDCC equations were solved by R -matrix method with variational method. The R -matrix method is very time consuming, especially when the number of channels is large. In the CDCC calculations for heavy weakly bound nuclei induced reactions, the number of channels is typically larger than 100 to well include the continuum coupling effect, which make R -matrix method very hard to use. Therefore, the finite-difference method based on Numerov algorithm [17] is adopted by us to solve the coupled channels equations, which permits fast integration of equations.

The aim of this paper is to show that the combination of the Lagrange mesh method and the finite-difference method based on Numerov algorithm can provide a suitable and efficient representation for the continuum states of a two body system and a quick calculation of CDCC equations. Three reactions are chosen to check the efficiency and accuracy of Lagrange mesh method in different cases: (i) $d+^{58}\text{Ni}$ at EL=80.0 MeV where d has no resonance state, (ii) $^6\text{Li}+^{40}\text{Ca}$ at EL=156.0 MeV in which ^6Li has D -wave resonance states and (iii) $^6\text{Li}+^{208}\text{Pb}$ at EL=33.0 MeV whose incident energy is around coulomb barrier. The CDCC results calculated with the momentum bin method will be the benchmark for comparison.

The paper is organized as follows. We briefly present the formalisms of CDCC, momentum bin method, Lagrange mesh method and breakup cross section calculation in section 2. Comparison between the CDCC with different discretization methods

for the three reactions are provided in section 3 to show the efficiency and accuracy of Lagrange mesh method. The summary and conclusion are presented in section 4 eventually.

2. Theoretical formalisms

2.1. Outline of CDCC

There are many literatures which have a detailed description of the CDCC theory [2,13]. Here we only present a brief introduction. The weakly bound nucleus is always the projectile in this paper and the spin of the target nucleus is ignored.

The weakly bound projectile is treated as two body system, consisting of a core particle (c) and a valence particle (v). Therefore the two-body Hamiltonian of the projectile is written as

$$H_P = T_{c-v} + V_{c-v}, \quad (1)$$

where T_{c-v} and V_{c-v} represent the relative motion kinetic energy and interaction of $c-v$ system respectively. The continuum states of the projectile are discretized into a finite number of states, which are regarded as the excited states to represent the continuum spectrum. The wave function for the projectile is expressed as

$$\begin{aligned} \phi_{l,j,I}^n &= \frac{\varphi_{l,j,I}^n(r)}{r} \left[[i^l Y_l(\Omega_r) \cdot s_v]_j \cdot s_c \right], 1 \leq n \leq N_{l,j,I}, \\ H_P \phi_{l,j,I}^n &= \varepsilon_{l,j,I}^n \phi_{l,j,I}^n, \end{aligned} \quad (2)$$

where the square bracket represents the angular momentum coupling. l is the orbital angular momentum for the $c-v$ relative motion. s_v and s_c are the spinor of v and c respectively. I is the angular momentum of projectile and it is formed by coupling j with s_c , where $\mathbf{j} = \mathbf{l} + \mathbf{s}_v$. $\varphi_{l,j,I}^n(r)$ is the radial wave function for $c-v$ system with relative coordinate r and it must be square-integrable for CDCC calculation. $N_{l,j,I}$ denotes the number of states with angular momentum coupling scheme (l, j, I) . $\varepsilon_{l,j,I}^n$ is the energy of $\phi_{l,j,I}^n$.

The excitation of the target nucleus is ignored. Therefore, the Hamiltonian of the target (H_T) is 0 and the total Hamiltonian of the three-body system ($c+v$ +target) is expressed as

$$\begin{aligned} H &= H_P + T_{P-T} + V_{c-T}(\vec{R} + f_c \vec{r}) + V_{v-T}(\vec{R} + f_v \vec{r}), \\ f_c &= \frac{m_v}{m_c + m_v}, f_v = -\frac{m_c}{m_c + m_v}, \end{aligned} \quad (3)$$

where T_{P-T} denotes the kinetic energy of projectile-target radial relative motion. V_{c-T} and V_{v-T} are the c -target and v -target interactions respectively, which are optical model potentials in general. R is the relative coordinate between the projectile and target. m_c and m_v are the mass of core and valence particles respectively. μ is the reduced mass

of system. In CDCC formalism, the total wave function is expanded over the projectile internal wave functions as

$$\Phi = \sum_{\beta, J} \frac{u_{\beta}^J(R)}{R} \psi_{\beta}^J, \psi_{\beta}^J = [i^L Y_L(\Omega_R) \otimes \phi_{l,j,I}^n]_J, \quad (4)$$

where u_{β}^J represents the projectile-target radial relative motion in β channel and the total angular momentum of system J . $\beta = \{n, l, j, I, L\}$. L is the orbital angular momentum for the projectile-target relative motion.

By projecting the schrodinger equation $H\Phi = E\Phi$ onto ψ_{β}^J , a set of coupled channels equations will be generated to determining u_{β}^J , that is

$$\left[\frac{\hbar^2}{2\mu} \left(-\frac{d^2}{dR^2} + \frac{L(L+1)}{R^2} \right) + V_{\beta, \beta}^J + \varepsilon_{\beta} - E \right] u_{\beta}^J = - \sum_{\beta' \neq \beta} V_{\beta, \beta'}^J u_{\beta'}^J, \quad (5)$$

where

$$V_{\beta, \beta'}^J = \langle \psi_{\beta}^J | V_{c-T} + V_{v-T} | \psi_{\beta'}^J \rangle. \quad (6)$$

ε_{β} is the projectile internal energy in the β channel. μ is the reduced mass of system. If V_{c-T} and V_{v-T} are only central potentials and rewritten by multipole expansion as

$$V_{c-T} + V_{v-T} = \sum_{\lambda} (2\lambda + 1) V_{\lambda}(R, r) P_{\lambda}(\cos \theta), \cos \theta = \Omega_R \cdot \Omega_r, \quad (7)$$

one can obtain the coupling matrix elements as

$$\begin{aligned} V_{\beta, \beta'}^J &= i^{L'+l'-L-l} (-1)^{s_c+s_v+l'+l+j+j'+I-I'-J} \hat{I} \hat{I}' \hat{J} \hat{J}' \hat{L} \hat{L}' \\ &\sum_{\lambda} (2\lambda + 1) \begin{Bmatrix} l' & j' & s_v \\ j & l & \lambda \end{Bmatrix} \begin{Bmatrix} j' & I' & s_c \\ I & j & \lambda \end{Bmatrix} \begin{Bmatrix} I' & L' & J \\ L & I & \lambda \end{Bmatrix} \\ &\times \begin{pmatrix} L' & \lambda & L \\ 0 & 0 & 0 \end{pmatrix} \begin{pmatrix} l' & \lambda & l \\ 0 & 0 & 0 \end{pmatrix} \int_0^{+\infty} \varphi_{l,j,I}^n V_{\lambda}(R, r) \varphi_{l',j',I'}^{n'} dr \end{aligned} \quad (8)$$

where $\hat{x} = \sqrt{2x+1}$. $3j$ and $6j$ symbols appear as usual. This expression of $V_{\beta, \beta'}^J$ is equivalent to those given in Ref. [18, 19], although the comparison requires some angular momentum algebra.

2.2. The momentum bin method

The momentum bin method [13, 14] generates the discretized state wave functions $\phi_{l,j}^n$ by dividing the continuum states $\{\phi_{l,j}^c(k, r); 0 < k < k_{max}\}$ into finite bins $\{[k_{i-1}, k_i]; 1 \leq i \leq N_{l,j}^c\}$ and then averaging continuum state wave function $\phi_{l,j,I}^c$ in each bin. That is

$$\begin{aligned} \phi_{l,j,I}^n &= \frac{1}{\sqrt{N_w}} \int_{k_{i-1}}^{k_i} w(k) \phi_{l,j,I}^c(k, r) dk, N_w = \int_{k_{i-1}}^{k_i} |w(k)|^2 dk, \\ n &= i + N_{l,j,I}^b, \end{aligned} \quad (9)$$

where $N_{l,j,I}^b$ is the number of bound states in angular momentum coupling scheme (l, j, I) and $N_{l,j,I}^b + N_{l,j,I}^c = N_{l,j,I}$. The weight function $w=1$ for non-resonance states and

$w = \sin \delta_l^{j,I}$ for resonance states [14, 19], where $\delta_l^{j,I}$ is the scattering phase shift for c - v system. Since $\langle \phi_{l,j,I}^c(k) | \phi_{l,j,I}^c(k') \rangle = \delta(k - k')$, the generated $\phi_{l,j,I}^n$ are mutually orthogonal as $\langle \phi_{l,j,I}^n | \phi_{l,j,I}^{n'} \rangle = \delta_{nn'}$.

2.3. Brief introduction of the Lagrange-mesh method

The Lagrange-mesh method is an approximate variational method and has been applied in many different physical fields [20]. Its basis functions and relative integration are associated with Gauss quadrature approximation and therefore a satisfying high accuracy can be obtained with small amount of computation.

For the half-infinite interval $[0, +\infty]$, regularized Lagrange-Laguerre mesh method (RLLM) is adopted and its N basis functions are defined as

$$f_i(r) = \frac{(-1)^i L_N(r/h)}{\sqrt{hx_i} r - hx_i} r e^{-hr/2}, \quad (10)$$

where L_N is the Laguerre polynomial of degree N and x_i are the zeros of L_N . h is a scaling parameter, adopted to the typical size of the system. These functions are used to diagonalize the Hamiltonian with Gauss quadrature [20] and generate a set of eigen functions φ_i .

$$\varphi_i = \sum_{j=1}^N c_j^i f_j. \quad (11)$$

The φ_i with negative eigenvalue ($\varepsilon_i < 0$) are used as the bound state radial wave functions and those with positive eigenvalue ($\varepsilon_i > 0$) are regarded as pseudo state radial wave functions. In practice, the φ_i with eigenvalue higher than energy cutoff value ($\varepsilon_i > \varepsilon_{max}$) will be omitted in CDCC calculations as high energy continuum states have little coupling effect in reactions.

The Lagrange condition reads

$$f_i(hx_j) = \frac{1}{\sqrt{h\lambda_j}} \delta_{i,j}, \quad (12)$$

where λ_j is the Gauss quadrature weight corresponding to x_j . The overlap and integration with local potential $V(r)$ can be obtained with Gauss quadrature efficiently as

$$\begin{aligned} \langle f_i | f_j \rangle &\approx \delta_{i,j}, \\ \langle f_i | V(r) | f_j \rangle &\approx V(hx_i) \delta_{i,j}. \end{aligned} \quad (13)$$

Therefore, the integration term in $V_{\beta,\beta'}$ can be calculated with a few potential values at the mesh points as

$$\int \varphi_i V \varphi_j dr = \sum_{k=1}^N c_k^i c_k^j V(hx_k). \quad (14)$$

The accuracy of the Gauss approximation in the Lagrange-mesh method has been discussed in many literatures, such as Ref. [20–22]. It is achieved especially when only the first few φ_i , whose eigenvalues are lower than others, are adopted to be the pseudo

state radial wave functions. Appropriate RLLM parameters will be given in section 3 to achieve convergence in CDCC calculations.

2.4. Breakup cross section calculation

Following the methods in Ref. [23], the scattering S -matrix from an entrance channel $\beta_0 = \{1, l_0, j_0, I_0, L_0\}$ to a breakup configuration with angular momentum coupling scheme $\gamma = \{l, j, I, L\}$ and wave number k can be approximated as

$$S_{\gamma, \beta_0}^J(k) = \sum_n \langle \phi_{l,j,I}^n | \phi_{l,j,I}^c(k) \rangle S_{\beta, \beta_0}^J. \quad (15)$$

The differential breakup cross section $d\sigma_{BU}/dk$ for the continuum states with angular momentum coupling scheme (l, j, I) is calculated as

$$\frac{d\sigma_{BU}(l, j, I)}{dk} = \frac{\pi}{K_0^2} \frac{1}{2I+1} \sum_{\beta_0 L J} (2J+1) |S_{\gamma, \beta_0}^J(k)|^2, \quad (16)$$

where K_0 is the projectile incident wave number. The breakup cross section can be obtained as

$$\sigma_{BU} = \sum_{l,j,I} \int \frac{d\sigma_{BU}(l, j, I)}{dk} dk. \quad (17)$$

The overlap in (15) is calculated numerically in RLLM, while it can be obtained analytically in momentum bin method as

$$\begin{aligned} \langle \phi_{l,j,I}^n | \phi_{l,j,I}^c(k) \rangle &= \frac{w(k)}{N_w}, k_{i-1} \leq k \leq k_i, \\ &= 0, \text{ else.} \end{aligned} \quad (18)$$

In order to effectuate this analytical result, a large radius where the bin wave functions are truncated (r_{bin}) is necessary for momentum bin method, especially when the calculated σ_{BU} and $d\sigma_{BU}/dk$ are converged.

Numerov algorithm is a well-known solution for coupled channel equations. Prof. Yang [17] provided a modified algorithm by using the iteration of the linear relationship between the radial wave functions at two neighboring points. This method can well improve the computational stability, which benefits the integration of CDCC equations significantly as the number of channels in CDCC is typically larger than those in other kinds of coupled channel calculations.

3. Applications of RLLM in CDCC

3.1. $d+^{58}\text{Ni}$ at $EL=80.0$ MeV

We firstly apply RLLM in the calculations for $d+^{58}\text{Ni}$ at $EL=80.0$ MeV, which has been variously studied in the past [2,5,23,24]. It would be a good test to check the correctness of our work. In the successful calculation by T. Druet et al. [16] for this reaction, the coupled channels equations were solved by R -matrix method with variational method. In that way, it was required to compute the inversion of a $N_{ch}N_{var}$ -dimensional matrix,

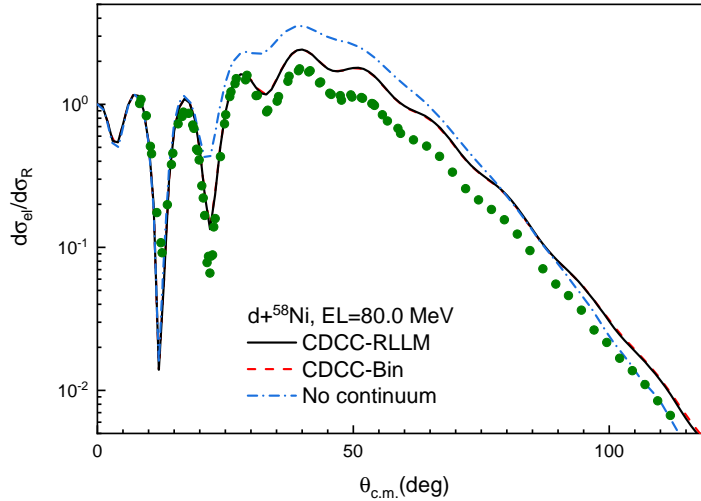


Figure 1. Calculated elastic scattering angular distribution in the Rutherford ratio for $d+^{58}\text{Ni}$ reaction at $EL=80.0$ MeV. The solid and dashed lines represent the CDCC-RLLM and CDCC-Bin results respectively. The dot-dashed line denotes the calculated results without continuum channels. The circles are the experimental data taken from Ref [26].

where N_{ch} is the number of channels and N_{var} is the number of basis functions used to solve coupled channels equations. As shown in Ref. [16], N_{var} should be 50 and 100 to obtain converged elastic scattering angular distribution and breakup cross section respectively.

In the finite-difference method based on Numerov algorithm [17], it is required to compute the inversion of a N_{ch} -dimensional matrix for $R_m/\Delta R$ times, where R_m is the asymptotic radius and ΔR is the step length. For this reaction, $R_m=20$ fm and $h=0.05$ fm are enough to obtain converged results. As the time complexity of the inversion for a M -dimensional matrix is $O(M^3)$, finite-difference method will be much faster than the R -matrix method ($R_m/\Delta R \ll N_{var}^3$) in solving coupled channels equations if N_{ch} is same for two methods.

We follow the work of Yahiro et al. [25], using the same potentials. Deuteron is composed of proton and neutron. The ground state of deuteron is restricted to be $1S$ state. S - and D -wave continuum states are included in CDCC calculations. The spins of proton and neutron are ignored so that $l=j=I$. The proton-target and neutron-target optical potentials are multipole expanded up to $\lambda=4$ for the calculations of $V_{\beta,\beta'}^J$. The procedure stops solving CDCC equations if the absorption from the elastic channel is less than 0.02 mb for three successive J sets. This stop condition is also used in the latter calculations.

For elastic scattering, the continuum states up to $k_{\max}=1.0$ fm $^{-1}$ are taken into calculations, which corresponds to $\varepsilon_{\max}=41.46$ MeV. The CDCC calculations with momentum bin method (CDCC-Bin) adopt the width of momentum bin $\Delta k=k_i - k_{i-1}=0.125$ fm $^{-1}$ and $r_{bin}=40$ fm, which are the same as the parameters in Ref [25]. $N=25$ and $h=0.4$ are used in the CDCC calculations with RLLM (CDCC-RLLM). With

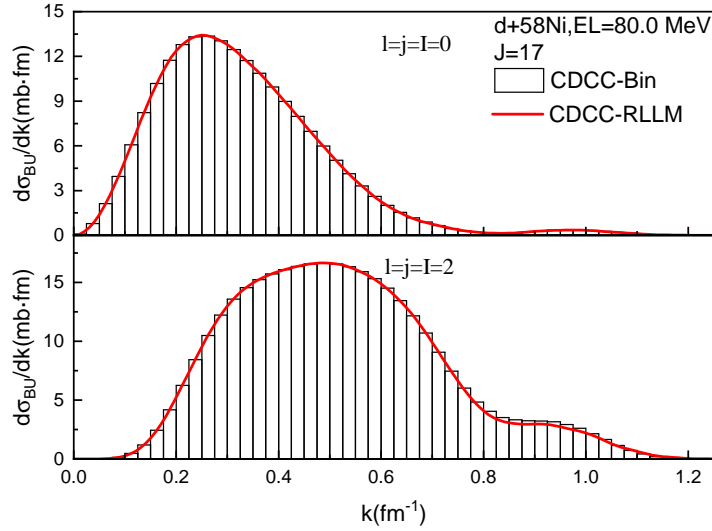


Figure 2. Calculated differential breakup reaction cross sections $d\sigma_{BU}/dk$ for $d+^{58}\text{Ni}$ reaction at $EL=80.0$ MeV at $J=17$. The histograms are the CDCC-Bin results and the solid lines represent the CDCC-RLLM results.

these parameters, $N_{0,0,0}=9$ and $N_{2,2,2}=8$ for CDCC-Bin, while $N_{0,0,0}=11$ and $N_{2,2,2}=10$ for CDCC-RLLM. Figure 1 shows the calculated elastic scattering angular distributions. The results of two methods are almost the same. Compared with the one-channel results, which were calculated without continuum channels, CDCC calculation improves the results in the angles from 25° to 80° . The discrepancy shows the sizable effect of coupling to the continuum states.

It is needed to include higher energy continuum states for breakup reaction calculations. k_{\max} is increased to be 1.25 fm^{-1} , corresponding to $\varepsilon_{\max}=64.78$ MeV. Finer discretization method is given to both two methods for converged $d\sigma_{BU}/dk$. CDCC-Bin uses $\Delta k=0.025 \text{ fm}^{-1}$ and $r_{bin}=100$ fm. CDCC-RLLM adopts $\{N = 60, h = 0.4\}$. We perform the calculations at $J=17$, where the partial breakup reaction cross section is the maximal. Satisfying agreement on $d\sigma_{BU}/dk$ is obtained for two discretization methods, as shown in figure 2. In this case, the number of states with $l=0$ and 2 are 51 and 50 for CDCC-Bin respectively, while they are 30 and 29 for CDCC-RLLM respectively. CDCC-RLLM can provide the same $d\sigma_{BU}/dk$ as those calculated by CDCC-Bin with less discretized states.

3.2. $^6\text{Li}+^{40}\text{Ca}$ at $EL=156.0$ MeV

The $^6\text{Li}+^{40}\text{Ca}$ reaction at $EL=156.0$ MeV is chosen to be the second example in this paper to perform CDCC calculations and ^6Li is treated as an $\alpha+d$ two body system. Different from the d induced reactions, the reactions induced by ^6Li are influenced severely by the D -wave resonance states of ^6Li . Therefore, this reaction will be a good test to assess the capacity of RLLM in dealing with the effect of resonance states.

Matsumoto et al. [23] has used this reaction to compare the momentum bin method

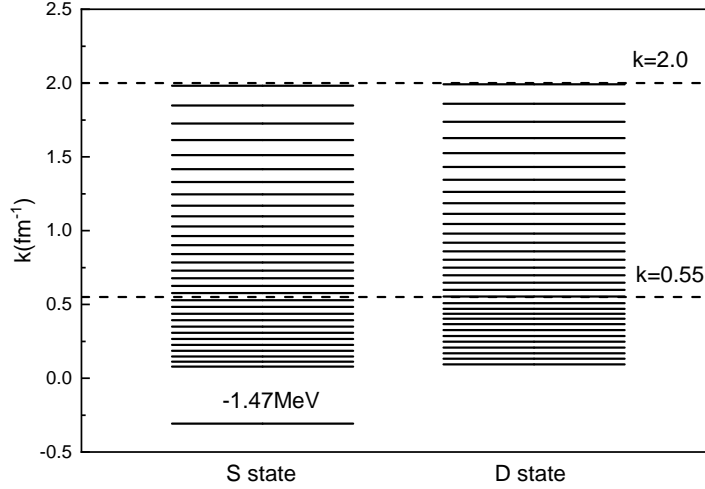


Figure 3. Discrete momentum of $\phi_{l,j,I}^n$ generated by RLLM for ${}^6\text{Li}$ with parameters $\{N = 50, h = 0.4\}$. The line with negative value corresponds to the bound state of ${}^6\text{Li}$. These discretized states are suitable for the calculation of ${}^6\text{Li}+{}^{40}\text{Ca}$ reaction at $EL=156$ MeV. See text for details.

and the PS method whose bases are a set of Gaussian functions, and good agreement was found on elastic scattering and breakup reaction. For the similar purpose, we perform CDCC calculations on the same reaction with moment bin method and RLLM for comparison. All adopted potentials are the same as those in Ref. [23]. $V_{\beta,\beta'}^J$ are calculated with α - ${}^{40}\text{Ca}$ and d - ${}^{40}\text{Ca}$ optical potentials multipole expanded up to $\lambda=4$. The ground state of ${}^6\text{Li}$ is assumed to be $2S$ configuration with binding energy 1.47 MeV. The spin of d is neglected for simplicity so that the triplet D -wave resonance states ($3^+, 2^+, 1^+$) is reduced to only one D -wave resonance state with resonance energy $\varepsilon_{res}=2.96$ MeV and resonance width $\Gamma_{res}=0.62$ MeV. Only the continuum states with $l=0$ and 2 are considered for CDCC calculations and they are truncated at $k_{max}=2.0$ fm^{-1} , corresponding to $\varepsilon_{max}=62.40$ MeV. The coupled channels equations are integrated up to $R_m=150$ fm with $\Delta R=0.03$ fm.

In CDCC-Bin calculations, we adopt the same discretization method as those in Ref. [23]. The D -wave continuum states are divided into two parts: resonance part ($0 \leq k \leq 0.55$ fm^{-1}) and non-resonance part ($0.55 \text{ fm}^{-1} \leq k \leq 2$ fm^{-1}). They are discretized into 30 and 20 bins respectively. In addition, the S -wave continuum states are divided into 20 bins. Therefore, $N_{0,0,0}=21$ and $N_{2,2,2}=50$. With these parameters, it is practical for all bins to use weight function $w=1$ and $r_{bin}=150$ fm to obtain converged elastic scattering angular distributions and breakup reaction cross sections simultaneously. For the same convergence ability, CDCC-RLLM adopts the parameters $\{N = 50, h = 0.4\}$. The number of generated states with $l=0$ and 2 are both 32. Figure 3 shows the momentum level of $\phi_{l,j,I}^n$ generated by RLLM for ${}^6\text{Li}$. It can be seen that discrete momentum are approximately equidistant below $k=0.55$ fm^{-1} and near linear distributed in $0.55 \text{ fm}^{-1} \leq k \leq 2$ fm^{-1} .

Same elastic scattering angular distributions are reproduced by CDCC-Bin and

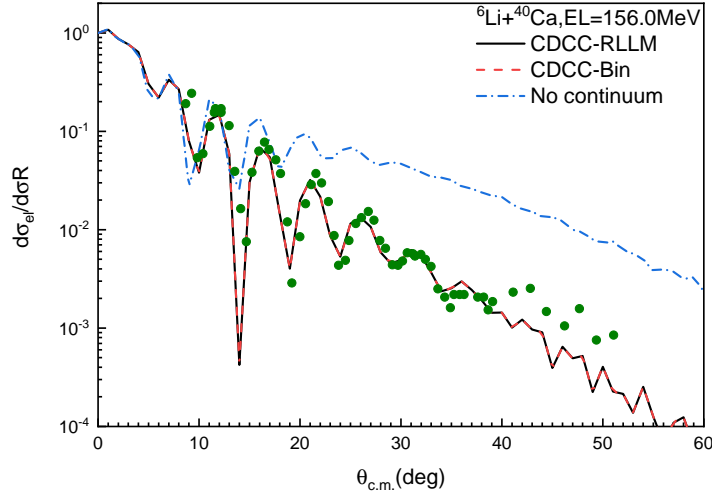


Figure 4. Same as figure 1 but for ${}^6\text{Li}+{}^{40}\text{Ca}$ at $EL=156.0$ MeV. Experimental data are taken from Ref. [27].

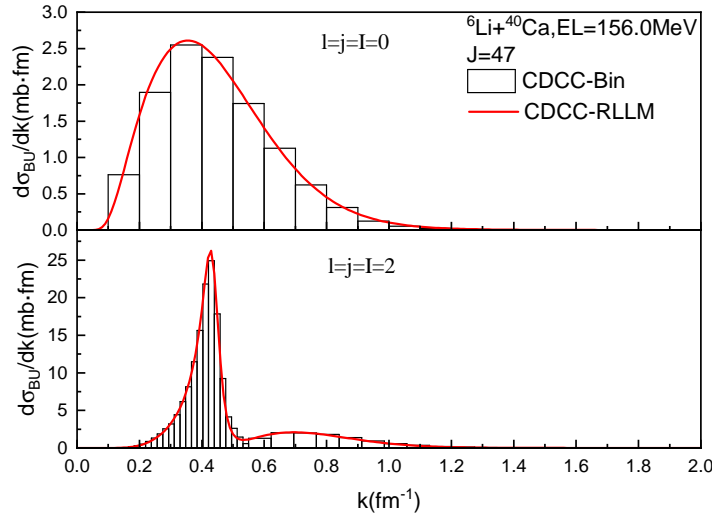


Figure 5. Same as figure 2 but for ${}^6\text{Li}+{}^{40}\text{Ca}$ at $EL=156.0$ MeV at $J=47$.

CDCC-RLLM as shown in figure 4. The one-channel calculation, whose continuum channels are omitted, is also included in the figure and it differs from the converged CDCC result notably. The divergence shows that the inclusion of breakup effect significantly improves the agreement with the experimental data.

In figure 5, the calculated $d\sigma_{BU}/dk$ from CDCC-Bin and CDCC-RLLM are presented at $J=47$, where the partial σ_{BU} reaches its maximum. Excellent agreement between two discretization methods are obtained. It is clearly observed that CDCC-Bin and CDCC-RLLM both well reproduce the prominent peak at $k=0.44$ fm^{-1} for D -wave continuum states, which arises from the simplified resonance state in $l=2$ continuum. As the number of states in CDCC-RLLM is about 90% of that in CDCC-Bin, it can be concluded that RLLM is an efficient method in describing the resonant states and its effect for scattering problems.

Table 1. Parameters of $V_{\alpha-d}$. $R_0=2.1$ fm and $a=0.65$ fm.

l	0	1	2
V_0^l (MeV)	67.69	63.90	65.33
$V_0^{so,l}$ (MeV)	0.00	5.72	4.78

Table 2. Calculated ε_{res}^{cal} and Γ_{res}^{cal} compared with experimental value ε_{res}^{exp} and Γ_{res}^{exp} [28].

state	ε_{res}^{cal} (MeV)	Γ_{res}^{cal} (MeV)	ε_{res}^{exp} (MeV)	Γ_{res}^{exp} (MeV)
3 ⁺	0.710	0.084	0.716	0.024
2 ⁺	3.00	1.12	2.84	1.30
1 ⁺	4.24	2.93	4.18	1.50

3.3. ${}^6\text{Li}+{}^{208}\text{Pb}$ at $EL=33.0$ MeV

We finally perform calculations on the reaction ${}^6\text{Li}+{}^{208}\text{Pb}$ at $EL=33.0$ MeV, whose incident energy is close to the coulomb barrier. In last decades, the reaction induced by weakly bound nuclei (such as ${}^6\text{Li}$) has extensively attract the interest of both experimental and theoretical physicists for nuclear physics research, and CDCC becomes a necessary study tool since the effect of coupling to continuum plays an important role in the reactions. Moreover, the coupling effect will be more significant when the incident energy is around the coulomb barrier. In this section, we not only test the validity of RLLM when EL is near the coulomb barrier, but also provide practicable parameters for the calculations of ${}^6\text{Li}$ induced reactions.

${}^6\text{Li}$ is still described in $\alpha + d$ cluster model. However, different from the example in section 3.2, continuum states with $l=0, 1$, and 2 are treated carefully here for CDCC calculations. α and d are regarded as the core and valence particles respectively. As the spin of α is zero, $j=I$. The interaction between clusters, $V_{\alpha-d}$, is chosen to be l -dependent in Woods-Saxon form.

$$\begin{aligned}
V_{\alpha-d}^l &= -V_0^l f(r) + V_0^{so,l} \frac{\lambda_\pi^2}{r} \frac{d}{dr} f(r) (\mathbf{l} \cdot \mathbf{s}) + V_C, \\
f(r) &= \frac{1}{1 + \exp\{(r - R_0)/a\}} \\
V_C &= Z_\alpha Z_d e^2 / r, r \geq R_0 \\
&= \frac{Z_\alpha Z_d e^2}{2R_0} \left(3 - \frac{r^2}{R_0^2} \right), r < R_0
\end{aligned} \tag{19}$$

where $\lambda_\pi^2=2.00$ fm². Z_α and Z_d are the charge number of α and d respectively. The parameters of $V_{\alpha-d}$ with $l=0, 1$ and 2 are listed in table 1. $V_{\alpha-d}$ can not only generate the binding energies for ${}^6\text{Li}$ correctly (1.47 MeV), but also can well reproduce the phase shifts for low-energy α - d scattering. Comparison between calculated phase shift and

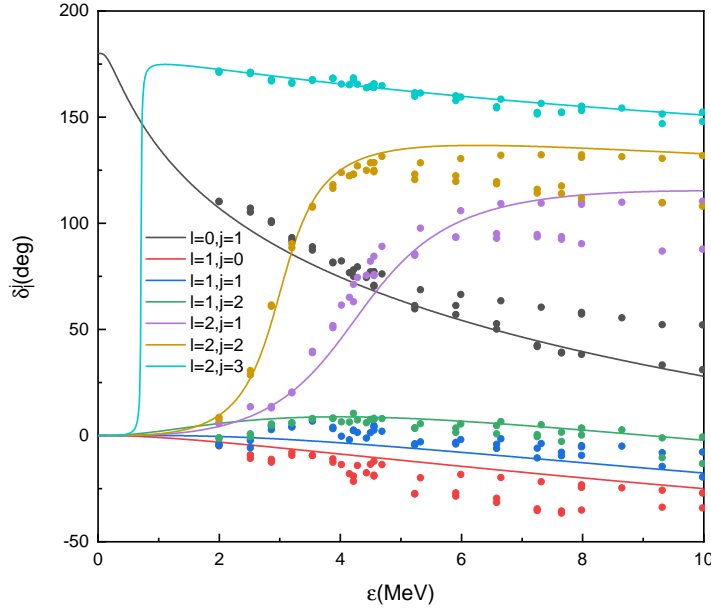


Figure 6. Calculated phase shift for α - d scattering compared with experimental data [29–31]. ε is the α - d relative energy in centre of mass system. $I=j$.

Table 3. $\varepsilon_{\min}^{(i)}$ and $\varepsilon_{\max}^{(i)}$ for ${}^6\text{Li}$ continuum states with $l=2$. $\varepsilon_{\min}^{(1)}=0$. $\varepsilon_{\max}^{(3)}=\varepsilon_{\max}$.

state	$\varepsilon_{\max}^{(1)}=\varepsilon_{\min}^{(2)}$ (MeV)	$\varepsilon_{\max}^{(2)}=\varepsilon_{\min}^{(3)}$ (MeV)
3^+	0.65	0.75
2^+	2.40	3.60
1^+	2.70	5.70

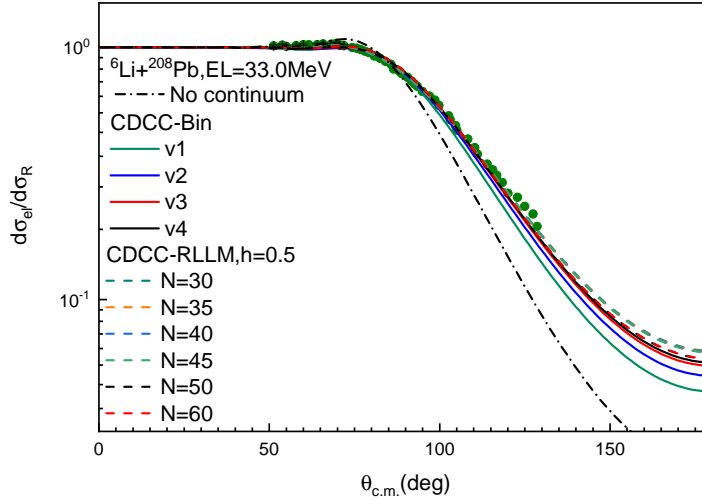
experimental data [29–31] are shown in figure 6. Calculated resonance energies ε_{res} and resonance widths Γ_{res} match the measured value [28] well as shown in table 2.

Different cutoff values of continuum state energy are adopted for elastic scattering and breakup reaction. In this section, h was optimized to be 0.5 fm for $V_{\alpha-d}$. We only vary N to change the discretized states and eliminate the eigen states with eigenenergies above ε_{max} .

It is necessary for the orthonormality of $\phi_{l,j,I}^n$ generated by momentum bin method to use different weight function w for resonance and non-resonance states as mentioned in section 2.2. Since there exist resonance states in $l=2$ continuum, each corresponding continuum is divided into three parts by energies ($[\varepsilon_{\min}^{(i)}, \varepsilon_{\max}^{(i)}]$, $i=1,2,3$) in momentum bin method. The boundary values of these energy interval are listed in table 3. All resonance states are located in the second intervals $[\varepsilon_{\min}^{(2)}, \varepsilon_{\max}^{(2)}]$. For other continuum states, there is only one energy interval: $\varepsilon_{\min}^{(1)}=0$, $\varepsilon_{\max}^{(1)}=\varepsilon_{max}$. As the continuum states are discretized equally with respect to k [13], it is convenient to determine the number of momentum bins in energy interval $[\varepsilon_{\min}^{(i)}, \varepsilon_{\max}^{(i)}]$ as $\lceil (\sqrt{\varepsilon_{\max}^{(i)}} - \sqrt{\varepsilon_{\min}^{(i)}})/d \rceil$, where $\lceil \dots \rceil$

Table 4. The parameters used to discretize continuum states for ${}^6\text{Li}$ with momentum bin method. The units of d_{res} and d_{no-res} are $\text{MeV}^{1/2}$.

	v1	v2	v3	v4	v5
d_{res}	0.75	0.50	0.25	0.15	0.0485
d_{no-res}	0.72	0.36	0.24	0.18	0.0485

**Figure 7.** Calculated elastic scattering angular distributions in the Rutherford ratio for ${}^6\text{Li}+{}^{208}\text{Pb}$ at $\text{EL}=33.0\text{MeV}$. The solid lines and dashed lines represent the CDCC-Bin and CDCC-RLLM results respectively. The dot-dashed line denotes the results calculated without continuum channels. The green circles are the experimental data taken from Ref. [34].

represents rounding up to an integer. d_{res} is used in $[\varepsilon_{\min}^{(2)}, \varepsilon_{\max}^{(2)}]$ for resonance continuum states and d_{no-res} in all other intervals.

The α and d optical potentials are taken from Refs. [32, 33] respectively and they are multipole expanded up to $\lambda=4$ for the calculations of $V_{\beta, \beta'}$. The incident energies of α and d are 22.0 MeV and 11.0 MeV respectively. For the d optical potential, the spin-orbital coupling term is ignored and the surface imaginary part is multiplied by 0.25.

In the elastic scattering calculations, the coupled channels equations are integrated up to $R_m=50$ fm with $\Delta R=0.05$ fm. ε_{max} is set to be 8.0 MeV since higher energies continuum states were found to have no effect on elastic scattering [35]. For CDCC-Bin, r_{bin} is set to be 100 fm for the convergence of $V_{\beta, \beta'}$ and four parameter sets (v1-v4) are used as shown in table 4. The calculated elastic scattering angular distributions are plotted in figure 7. As d_{res} and d_{no-res} decreasing, the number of discretized states increases and the calculated results rise in backward angle area. On the contrary, the calculated values of CDCC-RLLM decrease slightly when N increases from 30 to 50. The CDCC-RLLM results with $N=50$ are almost the same as those with $N=60$. It can be seen that both methods obtain almost same convergent result when the v4 parameters

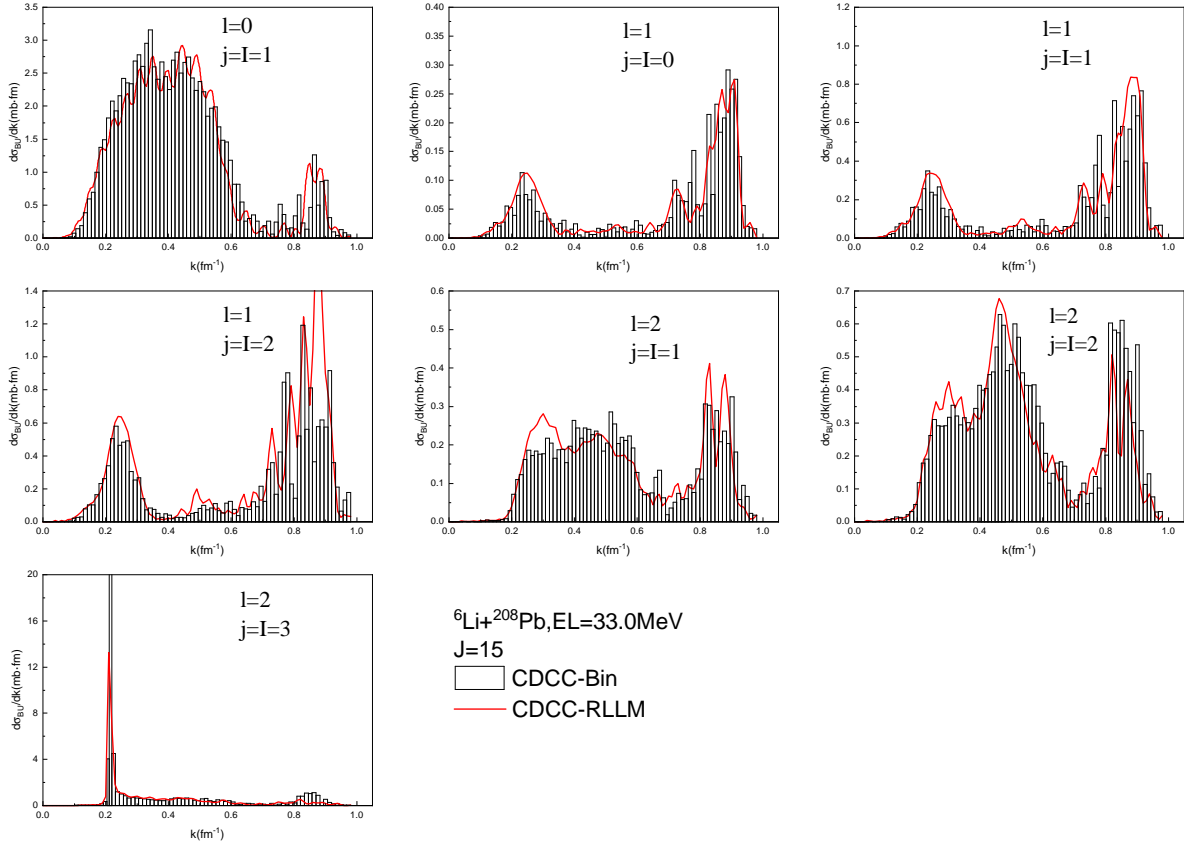


Figure 8. Differential breakup cross sections $d\sigma_{BU}/dk$ for ${}^6\text{Li}+{}^{208}\text{Pb}$ reaction at $EL=33.0$ MeV and $J=15$. The histograms are the CDCC-Bin results and the red lines represent the CDCC-RLLM results.

are used in CDCC-Bin and $\{N = 50, h = 0.5\}$ are adopted for CDCC-RLLM. With these parameters, the number of states in CDCC-Bin is 118 and that in CDCC-RLLM is 133. Both converged results are in excellent agreement with experiment data. In addition, we calculate the one-channel elastic scattering angular distributions without continuum channels and find that they are much smaller than the converged CDCC results above 90° . The agreement with the experimental data is improved observably by the effect of coupling to continuum states.

To achieve convergence in the calculation of σ_{BU} and $d\sigma_{BU}/dk$, a finer representation of continuum states and larger asymptotic radius are both needed by CDCC-Bin and CDCC-RLLM. ε_{max} is increased to be 15.0 MeV. For CDCC-RLLM, $R_m=150$ fm and $N=80$. Meanwhile, v5 parameters is adopted by CDCC-Bin, which are shown in table 4. R_m and r_{bin} are equally set to be 700 fm. These radii are well above $2\pi/\Delta k$, which ensures the normalization of all $\phi_{i,j,l}^n$ generated by momentum bin method.

The calculation of ${}^6\text{Li}$ breakup reaction is done at $J=15$, where partial breakup cross section is the largest. The σ_{BU} calculated by CDCC-Bin and CDCC-RLLM are 2.70 mb and 2.62 mb respectively, whose difference is less than 3%. Figure 8 shows the

differential breakup cross sections $d\sigma_{BU}/dk$ for each (l, j, I) . A narrow peak occurs in $d\sigma_{BU}/dk$ of $(l = 2, j = I = 3)$ at $k=0.21 \text{ fm}^{-1}$, which corresponds to the well-known 3^+ resonance state. Reasonable agreement is obtained in all cases, while the number of states in CDCC-RLLM is 271 and that in CDCC-Bin is 564. The efficiency of CDCC-RLLM to achieve convergence is much higher than CDCC-Bin in the calculations of ${}^6\text{Li}$ breakup reaction.

4. Summary and conclusion

We apply the regularized Lagrange-Laguerre mesh method (RLLM) to calculate the bound states and discretize the continuum states of weakly bound nuclei for continuum-discretized coupled-channels (CDCC) calculations. With the Gauss quadrature approximation, RLLM is shown to be an efficient and accurate discretization technique for the calculation of elastic scattering and breakup reaction. In the cases of $d+{}^{58}\text{Ni}$ at EL=80.0 MeV, ${}^6\text{Li}+{}^{40}\text{Ca}$ at EL=156.0 MeV and ${}^6\text{Li}+{}^{208}\text{Pb}$ at EL=33.0 MeV, the CDCC calculations with RLLM (CDCC-RLLM) are in excellent agreement with those with momentum bin method (CDCC-Bin), which is regarded as the standard discretization method. Moreover, the required number of states to achieve convergence in CDCC-RLLM is approximately equal to that of CDCC-Bin for elastic scattering and smaller for breakup reaction, which can well describe the sharp resonance peaks in ${}^6\text{Li}$ differential breakup reaction cross sections. This is a prominent advantage of RLLM. Particularly, in the reaction ${}^6\text{Li}+{}^{208}\text{Pb}$ at EL=33.0 MeV, where the long-range coulomb coupling effect is considerable and incident energy is around coulomb barrier, the required asymptotic radius and number of states in RLLM are much smaller than those in momentum bin method to obtain converged breakup cross sections, which shows the strong convergence capacity of RLLM.

In addition, a set of Woods-Saxon form potential for α - d system in S , P and D partial wave are given in the present paper, which can well describe the bound state of ${}^6\text{Li}$ and reproduce satisfying phase shifts of α - d scattering below 10 MeV. Practicable discretization method is provided based on RLLM for elastic scattering and breakup reaction and it will be used for our systematic study of ${}^6\text{Li}$ induced reactions in the future.

Finally, it is noted that RLLM could be extended for describing the bound and continuum states of three-body system in hyperspherical coordinate [20]. Therefore, it is worthy of applying RLLM in the study of reactions induced by three-body projectiles, such as ${}^6\text{He}(\alpha + 2n)$, ${}^{11}\text{Li}({}^9\text{Li}+2n)$ and ${}^9\text{Be}(2\alpha+n)$. Relative study is in progress.

Acknowledgments

This work was supported by the National Natural Science Foundation of China (11705009) and Science Challenge Project (TZ2018005).

References

- [1] Yahiro M, Matsumoto T, Minomo K, Sumi T and Watanabe S 2012 *Prog. Theor. Phys. Suppl.* **196** 87–101
- [2] Austern N, Iseri Y, Kamimura M, Kawai M, Rawitscher G and Yahiro M 1987 *Phys. Rep.* **154** 125–204
- [3] Sawada T and Thushima K 1986 *Prog. Theor. Phys.* **76** 440–459
- [4] Upadhyay N J, Deltuva A and Nunes F M 2012 *Phys. Rev. C* **85** 054621
- [5] Yahiro M, Iseri Y, Kameyama H, Kamimura M and Kawai M 1986 *Prog. Theor. Phys. Suppl.* **89** 32–83
- [6] Chau Hui-Tai P 2006 *Nucl. Phys. A* **773** 56–77
- [7] Mackintosh R S and Keeley N 2004 *Phys. Rev. C* **70** 024604
- [8] Tostevin J A, Nunes F M and Thompson I J 2001 *Phys. Rev. C* **63** 10
- [9] Camacho A G, Diaz-Torres A and Zhang H Q 2019 *Phys. Rev. C* **99** 1–7
- [10] Kamimura M, Matsumoto T, Hiyama E, Ogata K, Iseri Y and Yahiro M 2005 Continuum-discretized coupled-channels method for four-body breakup reactions *AIP Conf. Proc.* vol 791 pp 174–184
- [11] Summers N C, Nunes F M and Thompson I J 2006 *Phys. Rev. C* **74** 1–12
- [12] Gómez-Ramos M and Moro A M 2017 *Phys. Rev. C* **95** 1–10
- [13] Kawai M 1986 *Prog. Theor. Phys. Suppl.* **89** 11–31
- [14] Sakuragi Y, Yahiro M and Kamimura M 1986 *Prog. Theor. Phys. Suppl.* **89** 136–211
- [15] Druet T, Baye D, Descouvemont P and Sparenberg J M 2010 *Nucl. Phys. A* **845** 88–105
- [16] Druet T and Descouvemont P 2012 *Eur. Phys. J. A* **48** 1–10
- [17] Yang Z 1980 *Chinese Phys. C* **4** 374
- [18] Nishioka H, Tostevin J A, Johnson R C and Kubo K I 1984 *Nucl. Phys. A* **415** 230–270
- [19] Thompson I J 1988 *Computer Physics Reports* **7** 167–212 ISSN 0167-7977
- [20] Baye D 2015 *Phys. Rep.* **565** 1–107
- [21] Baye D 2011 *J. Phys. A Math. Theor.* **44** 395204
- [22] Baye D, Hesse M and Vincke M 2002 *Phys. Rev. E* **65** 026701
- [23] Matsumoto T, Kamizato T, Ogata K, Iseri Y, Hiyama E, Kamimura M and Yahiro M 2003 *Phys. Rev. C* **68** 10
- [24] Moro A M, Arias J M, Gómez-Camacho J and Pérez-Bernal F 2009 *Phys. Rev. C* **80** 1–10
- [25] Yahiro M, Nakano M, Iseri Y and Kamimura M 1982 *Prog. Theor. Phys.* **67** 1467–1482
- [26] Stephenson E J, Collins J C, Foster C C, Friesel D L, Jacobs W W, Jones W P, Kaitchuck M D, Schwandt P and Daehnick W W 1983 *Phys. Rev. C* **28**(1) 134–140
- [27] Majka Z, Gils H J and Rebel H 1978 *Zeitschrift für Phys. A Atoms Nucl.* **288** 139–152
- [28] Tilley D, Cheves C, Godwin J, Hale G, Hofmann H, Kelley J, Sheu C and Weller H 2002 *Nucl. Phys. A* **708** 3–163
- [29] Grüebler W, Schmelzbach P, König V, Risler R and Boerma D 1975 *Nucl. Phys. A* **242** 265–284
- [30] Jenny B, Grüebler W, König V, Schmelzbach P and Schweizer C 1983 *Nucl. Phys. A* **397** 61–101
- [31] Schmelzbach P, Grüebler W, König V and Marmier P 1972 *Nucl. Phys. A* **184** 193–213
- [32] Avrigeanu V, Avrigeanu M and Manaiescu C 2014 *Phys. Rev. C* **90** 044612
- [33] An H and Cai C 2006 *Phys. Rev. C* **73** 054605
- [34] Keeley N, Bennett S, Clarke N, Fulton B, Tungate G, Drumm P, Nagarajan M and Lilley J 1994 *Nucl. Phys. A* **571** 326–336
- [35] Keeley N and Rusek K 1998 *Phys. Lett. B* **427** 1–6